Supplementary Material for "Understanding the role of Sn substitution and Pb-□ in enhancing the optical properties and solar cell efficiency of $CH(NH_2)_2Pb_{1-X-Y}Sn_X\square_YBr_3$"

Manjari Jain*, Arunima Singh, Pooja Basera, Manish Kumar, Saswata Bhattacharya*
Department of Physics, Indian Institute of Technology Delhi, New Delhi 110016, India
(Dated: May 15, 2020)

Thermodynamic stability computed with HSE06 functional

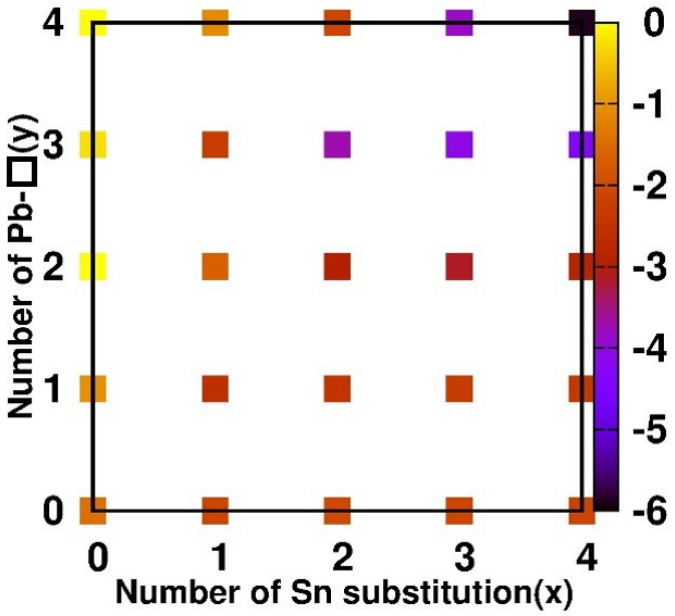

Figure S1: Computed energetics for $FAPb_{1-x-y}Sn_x\square_yBr_3$ using HSE06 functional.

The HSE06 functional provides the same thermodynamic stability trend as HSE06+SOC. However, the values of formation energy is more negative with HSE06+SOC, as compared to HSE06. HSE06+SOC is considered for further study as it is more accurate. The formation energy plot with HSE06 function is shown in Fig. S1

Goldschmidt tolerance factor t and octahedral factor μ for the stable perovskite structure

The Goldschmidt tolerance factor t is evaluated using the following expression : $t = \frac{r_A + r_X}{\sqrt{2}(r_B + r_X)}$

Octahedral factor μ is defined as: $\mu = \frac{r_B}{r_X}$

where r_A, r_B, r_X are the ionic radii of A, B cation and X anion, respectively.

For stable cubic perovskite, the tolerance factor t should be in the range of $0.813 \leq t \leq 1.107$, and the octahedral factor should be lie in between $0.377 \leq \mu \leq 0.895$ [1, 2].

* Manjari.Jain@physics.iitd.ac.in [MJ], saswata@physics.iitd.ac.in [SB]

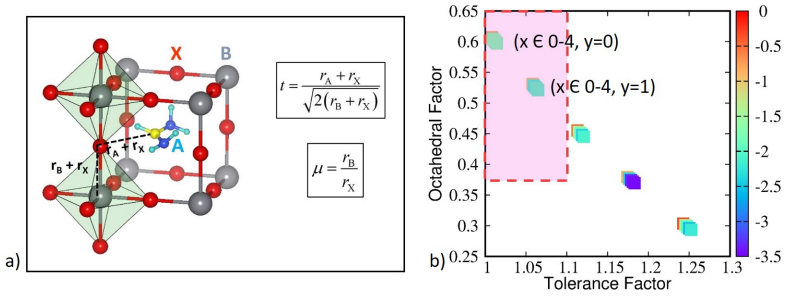

Figure S2: (a)Schematic representation of atomic structure of $FAPbBr_3$ perovskite: defining tolerance factor and octahedral factor. (b) 2D view of 3D plot, where in x-axis tolerance factor t, and in y-axis Octahedral factor μ. The color bar show the formation energy (z-axis) of $FA_8Pb_{8-x-y}Sn_x\square_yBr_{24}$. Variation of x and y are given in the plot. The dotted line show the region where conformers obey the structure stability. The shaded portion show the most stable conformers, that follow structure stability as well as thermodynamic stability.

TABLE S1: Goldschmidt tolerance factor t and octahedral factor μ for all the conformers.

$FA_8Pb_{8-x-y}Sn_x\square_yBr_{24}$ conformers	t	μ
x=0, y=0	1.007	0.607
x=1, y=0	1.009	0.604
x=2, y=0	1.011	0.602
x=3, y=0	1.012	0.599
x=4, y=0	1.014	0.597
x=0, y=1	1.057	0.531
x=1, y=1	1.059	0.528
x=2, y=1	1.061	0.526
x=3, y=1	1.063	0.523
x=4, y=1	1.064	0.521
x=0, y=2	1.113	0.455
x=1, y=2	1.114	0.452
x=2, y=2	1.117	0.450
x=3, y=2	1.119	0.448
x=4, y=2	1.121	0.445
x=0, y=3	1.174	0.378
x=1, y=3	1.176	0.377
x=2, y=3	1.178	0.374
x=3, y=3	1.181	0.372
x=4, y=3	1.183	0.369
x=0, y=4	1.242	0.303
x=1, y=4	1.245	0.301
x=2, y=4	1.247	0.298
x=3, y=4	1.249	0.259
x=4, y=4	1.252	0.293

Radial Distribution Function at T = 0K and T = 300K for $FA_8Pb_{8-x}Sn_xBr_{24}$

The radial distribution function (g(r)) is an important structural characteristic. The structural stability of different stable defect configurations are also checked at higher temperature using *ab initio* molecular dynamics (AIMD). We have obtained the plot for g(r) at T = 0K and T = 300K. We observe that, the nature of the radial distribution function remains same at room temperature for the nearest neighbours.

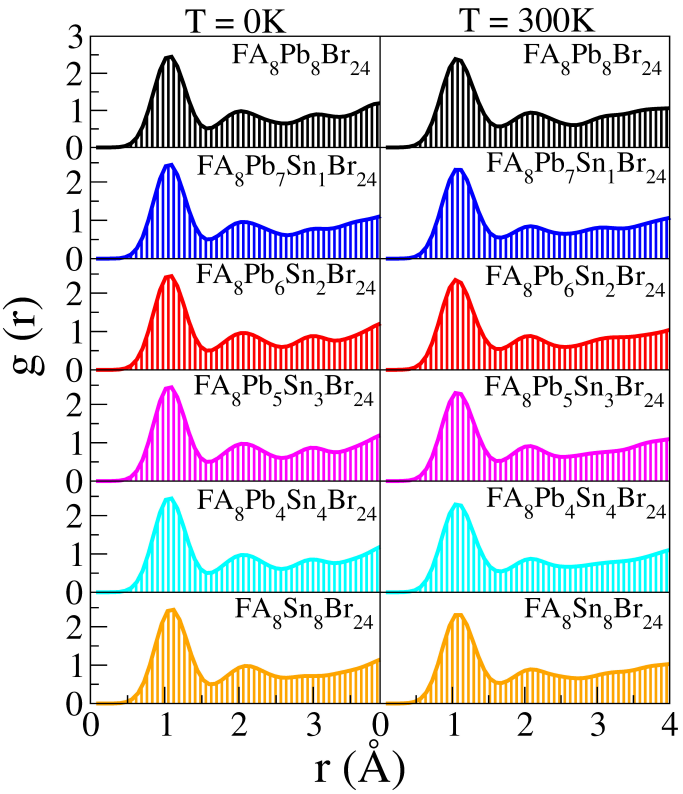

Figure S3: Radial distribution function for different stable phases of $FA_8Pb_{8-x}Sn_xBr_{24}$ at T = 0K and T = 300K

Electronic structure of pure and mixed $FAPb_{1-x}Sn_xBr_3$ perovskites

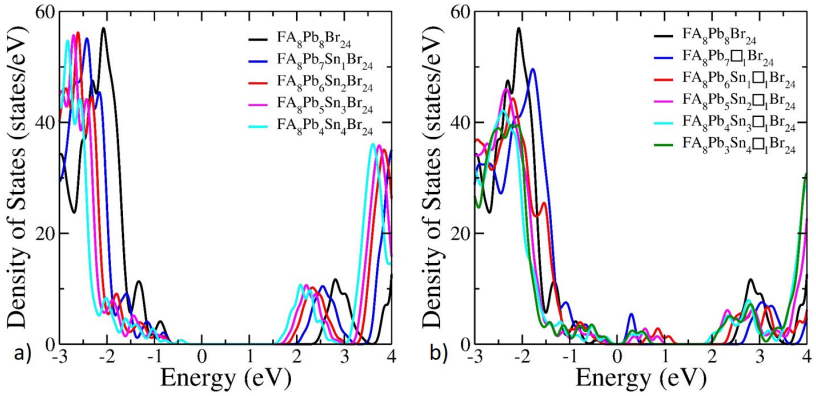

Figure S4: Density of states (DOS) of (a) $FA_8Pb_{8-x}Sn_xBr_{24}$ and (b) $FA_8Pb_{7-x}Sn_x\square_1Br_{24}$ as calculated by HSE06.

We have plotted the density of states (DOS) for $FA_8Pb_{8-x}Sn_xBr_{24}$ (Fig. S4(a)), to better understand the role of Pb-□ and Sn substitution in enhancing the efficiency of $FAPbBr_3$. The results show that, as the Sn concentration increases, the valence bands (VBs) shift away from the Fermi-level, whereas the VBM remains at the same position. On the other hand, with increase in Sn concentration the CBm shifts toward the Fermi-level as shown in Fig. S4(a). Also, we have plotted the DOS for $FA_8Pb_{7-x}Sn_x\square_1Br_{24}$ (Fig. S4(b)). This shows that the creation of a Pb-□ results in the formation of a shallow state. As Sn substitution is introduced with Pb-□, trap states are formed that act as recombination centres, resulting in degradation of the optoelectronic performance. Also, these defect configuration gives indirect bandgap. Hence, Sn substitution with one Pb-□ fails to be applicable in the photovoltaics. So, only $FA_8Pb_{8-x}Sn_xBr_{24}$ conformers are taken for further optical studies.

Effect of Sn substitution on the band-gap of $FAPb_{8-x}Sn_xBr_3$ and Absorption coefficient using HSE06

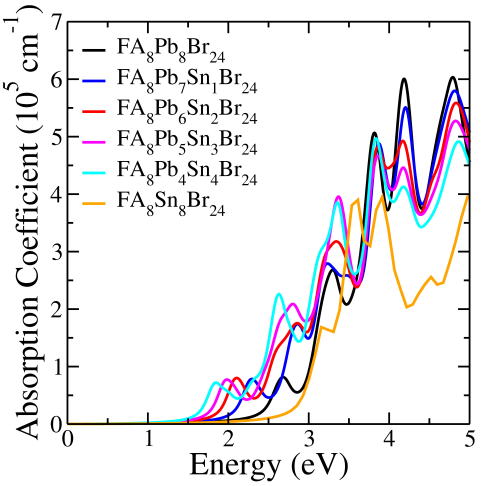

Figure S5: Absorption coefficient using HSE06.

TABLE S2: Bandgap using HSE06

Conformers	Bandgap (eV)
$FA_8Pb_8Br_{24}$, (x=0)	2.50
$FA_8Pb_7Sn_1Br_{24}$, (x=1)	2.24
$FA_8Pb_6Sn_2Br_{24}$, (x=2)	2.05
$FA_8Pb_5Sn_3Br_{24}$, (x=3)	1.93
$FA_8Pb_4Sn_4Br_{24}$, (x=4)	1.80
$FA_8Sn_8Br_{24}$, (x=8)	2.86

The x and y values for the conformers $FA_8Pb_{8-x-y}Sn_x\square_yBr_{24}$ are $x \in [0,4]$ and $y = 0$. For Pb-$\square$, the bandgap is indirect. Hence, we consider only $y = 0$ and $x \in [1,4]$. It is to be noted that the bandgap value is overestimated.

Optical properties and SLME calculation using PBE

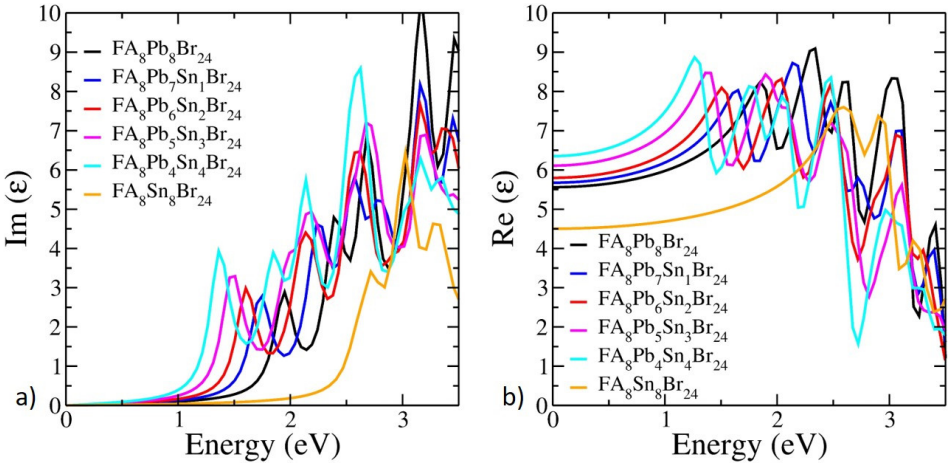

Figure S6: (a) Imaginary part of the dielectric function Im(ε) and, (b) Real part of the dielectric function Re(ε) calculated using PBE.

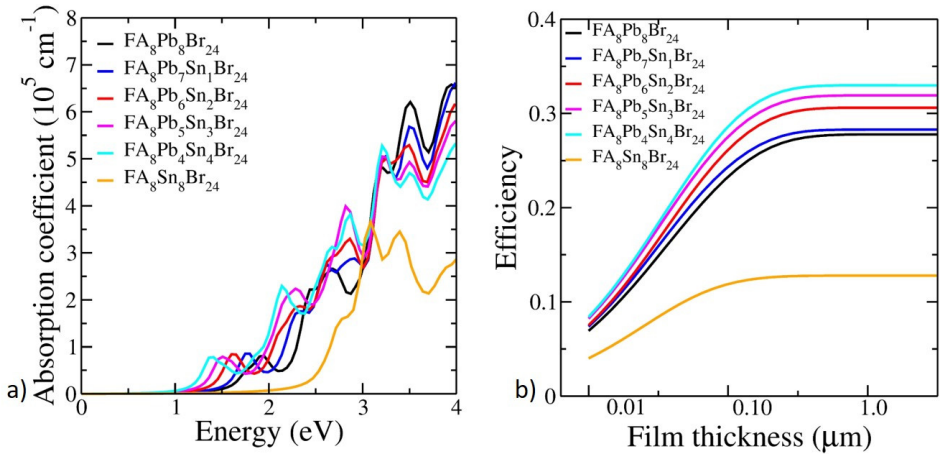

Figure S7: (a) Absorption coefficient and, (b) SLME as function of film thickness using PBE.

We have plotted the imaginary Im(ε) and real Re(ε) part of the dielectric function using PBE (Fig. S6(a) and (b)). The nature of the graph is similar to the obtained by HSE06. Further, we have plotted the absorption spectra and SLME for different defect conformers $FA_8Pb_{8-x}Sn_xBr_{24}$ (Fig. S7(a) and (b)). The SLME value for different defect conformers is listed in below table S3.

TABLE S3: SLME using PBE

Conformers	SLME (%)
$FA_8Pb_8Br_{24}$, (x=0, y=0)	27.80
$FA_8Pb_7Sn_1Br_{24}$, (x=1, y=0)	28.20
$FA_8Pb_6Sn_2Br_{24}$, (x=2, y=0)	30.60
$FA_8Pb_5Sn_3Br_{24}$, (x=3, y=0)	31.91
$FA_8Pb_4Sn_4Br_{24}$, (x=4, y=0)	32.98
$FA_8Sn_8Br_{24}$, (x=8, y=0)	12.78

Using PBE, the value of bandgap is underestimated. Hence, the value of SLME is quite high in comparison to the HSE06 values. It is to be noted that the trend of SLME efficiency is quite same as that of HSE06.

References

[1] C. Li, K. C. K. Soh and P. Wu, *Journal of alloys and compounds*, 2004, **372**, 40–48.
[2] C. Li, X. Lu, W. Ding, L. Feng, Y. Gao and Z. Guo, *Acta Crystallographica Section B: Structural Science*, 2008, **64**, 702–707.